The Sloan Digital Sky Survey Quasar Catalog I. Early Data Release [1]

Donald P. Schneider[2], Gordon T. Richards[2], Xiaohui Fan[3], Patrick B. Hall[4,5],
Michael A. Strauss[4], Daniel E. Vanden Berk[6], James E. Gunn[4], Heidi Jo Newberg[7],
Timothy A. Reichard[2], C. Stoughton[6], Wolfgang Voges[8], Brian Yanny[6], Scott F. Anderson[9],
James Annis[6], Neta A. Bahcall[4], Amanda Bauer[10], Mariangela Bernardi[11], Michael R. Blanton[6],
William N. Boroski[6], J. Brinkmann[12], John W. Briggs[11], Robert Brunner[13], Scott Burles[11],
Larry Carey[9], Francisco J. Castander[14], A.J. Connolly[15], István Csabai[16,17], Mamoru Doi[18],
Scott Friedman[16], Joshua A. Frieman[11], Masataka Fukugita[19,3], Timothy M. Heckman[16],
G.S. Hennessy[20], Robert B. Hindsley[21], David W. Hogg[3], Željko Ivezić[4], Stephen Kent[6],
Gillian R. Knapp[4], Peter Z. Kunszt[16], Donald Q. Lamb[11,22], R. French Leger[9], Daniel C. Long[12],
Jon Loveday[23], Robert H. Lupton[4], Bruce Margon[24], Avery Meiksin[25], Aronne Merelli[13],
Jeffrey A. Munn[26], Matthew Newcomb[27], R.C. Nichol[27], Russell Owen[9], Jeffrey R. Pier[26],
Adrian Pope[27], Constance M. Rockosi[11], David H. Saxe[3], David Schlegel[4], Walter A. Siegmund[9],
Stephen Smee[16], Yehuda Snir[27], Mark SubbaRao[11], Alexander S. Szalay[16],
Aniruddha R. Thakar[16], Alan Uomoto[16], Patrick Waddell[9], and Donald G. York[11,22]

[2]Department of Astronomy and Astrophysics, The Pennsylvania State University, University Park, PA 16802.

[3]The Institute for Advanced Study, Princeton, NJ 08540.

[4]Princeton University Observatory, Princeton, NJ 08544.

[5]Pontificia Universidad Católica de Chile, Departamento de Astronomía y Astrofísica, Facultad de Física, Casilla 306, Santiago 22, Chile.

[6]Fermi National Accelerator Laboratory, P.O. Box 500, Batavia, IL 60510.

[7]Department of Physics, Applied Physics and Astronomy, Rensselaer Polytechnic Institute, Troy, NY 12180.

[8]Max-Planck-Institute für extraterrestrische Physik, Geissenbachstr. 1, D-85741 Garching, Germany.

[9]University of Washington, Department of Astronomy, Box 351580, Seattle, WA 98195.

[10]Department of Physics, University of Cincinnati, 400 Physics Bldg., Cincinati, OH 45221.

[11]Astronomy and Astrophysics Center, University of Chicago, 5640 South Ellis Avenue, Chicago, IL 60637.

[12]Apache Point Observatory, P.O. Box 59, Sunspot, NM 88349-0059.

[13]Astronomy Department, California Institute of Technology, Pasadena, CA 91125.

[14]Universidad de Chile, Casilla 36-D, Santiago, Chile.

[15]Department of Physics and Astronomy, University of Pittsburgh, 3941 O'Hara Street, Pittsburgh, PA 15260.

[16]Department of Physics and Astronomy, The Johns Hopkins University, 3701 University Drive, Baltimore, MD 21218.

[17]Department of Physics of Complex Systems, Eötvös University, Pázmáy Péter sétány 1/A, H-1117, Budapest, Hungary.

[18]Department of Astronomy and Research Center for the Early Universe, School of Science, University of Tokyo, Mitaka, Tokyo 181-0015, Japan.

[19]Institute for Cosmic Ray Research, University of Tokyo, Kashiwa, 2778582, Japan.

[20]US Naval Observatory, 3450 Massachusetts Avenue NW, Washington, DC 20392-5420.

[21]Remote Sensing Division, Code 7215, Naval Research Laboratory, 4555 Overlook Ave. SW, Washington, DC 20375.

[22]The University of Chicago, Enrico Fermi Institute, 5640 South Ellis Avenue, Chicago, IL 60637.

[23]Astronomy Centre, University of Sussex, Falmer, Brighton BN1 9QJ, UK.

[24]Space Telescope Science Institute, 3700 San Martin Drive, Baltimore, MD 21218.

[25] Royal Observatory, Edinburgh, Blackford Hill, Edinburgh EH9 3HJ, UK.

[26]US Naval Observatory, Flagstaff Station, P.O. Box 1149, Flagstaff, AZ 86002-1149.

[27]Dept. of Physics, Carnegie Mellon University, 5000 Forbes Ave., Pittsburgh, PA 15232.

ABSTRACT

We present the first edition of the Sloan Digital Sky Survey (SDSS) Quasar Catalog. The catalog consists of the 3814 objects (3000 discovered by the SDSS) in the initial SDSS public data release that have at least one emission line with a full width at half maximum larger than 1000 km s^{-1}, luminosities brighter than $M_{i*} = -23$, and highly reliable redshifts. The area covered by the catalog is 494 deg^2; the majority of the objects were found in SDSS commissioning data using a multicolor selection technique. The quasar redshifts range from 0.15 to 5.03. For each object the catalog presents positions accurate to better than 0.2″ rms per coordinate, five band ($ugriz$) CCD-based photometry with typical accuracy of 0.05 mag, radio and X-ray emission properties, and information on the morphology and selection method. Calibrated spectra of all objects in the catalog, covering the wavelength region 3800 to 9200 Å at a spectral resolution of 1800-2100, are also available. Since the quasars were selected during the commissioning period, a time when the quasar selection algorithm was undergoing frequent revisions, the sample is not homogeneous and is not intended for statistical analysis.

Subject headings: catalogs, surveys, quasars:general

1. Introduction

Since the first measurement of a quasar redshift nearly 40 years ago (Schmidt 1963), the number of known quasars has steadily risen; the NASA/IPAC Extragalactic Database (NED) and the quasar catalog of Véron & Veron (2001) each contain on the order of 25,000 quasars. A large fraction of these objects were recently discovered by the 2dF Quasar Survey (Croom et al. 2001), which is extremely effective at identifying quasars with redshifts below 3.0 that have b_J magnitudes between 18.25 and 20.85.

This paper presents the first edition of the Sloan Digital Sky Survey (SDSS) Quasar Catalog. The goal of the SDSS quasar survey is to obtain spectra of $\approx$ 100,000 quasars from 10,000 deg^2 of the North Galactic Cap. For quasars with $(u - g) < +1.5$ (which corresponds to a redshift of near three), the survey will reach a flux limit of $i \approx 19$; quasars with $(u - g) > +1.5$ (corresponding to a redshift range in the SDSS of between 3.0 and $\approx$ 5.5-6.0), the sensitivity limit will be $i \approx 20$. The survey will provide CCD-based photometry in five broad bands covering the entire optical window, morphological information, and spectra from 3800 Å to 9200 Å at a spectral resolution of 1800-2100. A review of the SDSS is given by York et al. (2000); Richards et al. (2002) present the details of the quasar target algorithm.

The catalog in the present paper consists of the 3814 objects in the SDSS Early Data Release (EDR; Stoughton et al. 2002) with reliable redshifts whose spectra have at least one emission line with a FWHM broader than 1000 km s^{-1} and which have a luminosity larger than $M_{i*} = -23$ (calculated assuming an $H_0 = 50$ km s^{-1} Mpc^{-1}, $\Omega_M = 1.0$, $\Omega_\Lambda = 0$ cosmology, which will be used throughout this paper). The quasars range in redshift from 0.15 to 5.03, and 3000 (79%) were discovered by the SDSS (an object is classified as previously known if NED contains a quasar within 5″ of the SDSS position).

A few quasar-related studies based on subsets of the SDSS Early Release Data have been recently published. The most comprehensive investigations, both using samples containing more than 2000 quasars, are the quasar color-redshift relation for redshifts between zero and five (Richards et al. 2001a) and the construction of a very high signal-to-noise ratio composite quasar spectrum (Vanden Berk et al. 2001). The SDSS has proven to be extremely effective at identifying high-redshift quasars; to date the SDSS has discovered more than 140 at redshifts above four, and ten of the eleven known quasars at $z \geq 5$ (see Zheng et al. 2000, Anderson et al. 2001, Fan et al. 2001, and references therein; the sole non-SDSS $z > 5$ quasar is described in Sharp et al. 2001).

The observations used to produce the catalog are presented in Section 2. The construction of the catalog and the catalog format are discussed in Sections 3 and 4, respectively, and Section 5 contains a summary of the catalog. A brief discussion of plans for future editions of the catalog is given in Section 6. The catalog material can be found at a public web site [28].

2. Observations

2.1. Sloan Digital Sky Survey

The Sloan Digital Sky Survey uses a CCD camera (Gunn et al. 1998) on a dedicated 2.5-m telescope at Apache Point Observatory, New Mexico, to obtain images in five broad optical bands over 10,000 deg^2 of the high Galactic latitude sky centered approximately on the North Galactic Pole. The five filters (designated u, g, r, i, and z) cover the entire wavelength range of the CCD response (Fukugita et al. 1996); the filter response curves are given in Stoughton et al. (2002). Since the SDSS photometric system is not yet finalized, we refer to the SDSS photometry presented here as u^*, g^*, r^*, i^*, and z^*. The photometric calibration is reproducible to 0.05, 0.03, 0.03, 0.03, and 0.05 magnitudes in u^*, g^*, r^*, i^*, and z^*, respectively; the absolute calibration in Janskys is uncertain at the 10% level. All magnitudes in the quasar catalog refer to the point spread function measurements of the photometric pipeline (see Stoughton et al. 2002 for details).

Photometric calibration is provided by simultaneous observations with a 20-inch telescope at the same site (see Hogg et al. 2001 and Stoughton et al. 2002). The survey data processing

---

[28]http://archive.stsci.edu/sdss/documents/prepared_ds.html

software measures the properties of each detected object in the imaging data in all five bands, and determines and applies both astrometric and photometric calibrations (Pier et al., unpublished; Lupton et al. 2001). The image quality in the EDR, which consists of observations taken during the SDSS commissioning period, is considerably poorer than that expected for the survey proper; the 95% completeness limits for stars in the EDR are typically 22.0, 22.2, 22.2, 21.3, and 20.5 in u^*, g^*, r^*, i^* and z^*, respectively. The image of an unresolved source brighter than $r^* \approx 14$ will be saturated.

The imaging data in the SDSS EDR consists of eight imaging scans (SDSS scan numbers 94, 125, 752, 756, 1336, 1339, 1356, and 1359), acquired between September 1998 and April 2000, that cover approximately 500 deg^2. The first four scans are along the celestial equator in the Northern and Southern high-latitude Galactic sky; the final four contain 68 deg^2 in the SIRTF First Look Survey region (see Stoughton et al. 2002).

2.2. Target Selection

The SDSS filter system was designed to allow quasars at redshifts between zero and six to be identified with multicolor selection techniques. The effective wavelength of the u filter is shortward of the Balmer discontinuity; therefore the color difference between low-redshift quasars and early-type stars is larger in $(u - g)$ than the standard color of $(U - B)$. The inclusion of the near-infrared filter (z) extends the maximum redshift for SDSS quasars out to ≈ 6 (Fan et al. 2001). The vast majority of quasars follow a tight color-redshift relation in SDSS filters (Richards et al. 2001a); this feature allows development of techniques that may produce reliable photometric redshifts for quasars (Richards et al. 2001b, Budavari et al. 2001). In addition to the multicolor selection, unresolved objects brighter than $i \approx 19$ that are coincident with FIRST radio sources (Becker, White, & Helfand 1995) are also identified as quasar candidates.

Note that the point spread function magnitudes are used for the quasar target selection. For candidates whose likely redshifts are less than three, both extended and point sources are included as quasar candidates; however, extended sources are excluded if they lie in a region of color space that is densely occupied by normal galaxies (see Richards et al. 2002). At larger redshifts, an object must be unresolved in the SDSS images to become a spectroscopic target.

Target selection also imposes a maximum brightness limit on the objects. Accurate photometry of point sources brighter than $r \approx 14$ is impossible as their images are saturated; objects that have saturated pixels are dropped from further consideration. An additional constraint is introduced to prevent saturation and fiber cross-talk problems in the SDSS spectroscopic observations; an object cannot be included in the quasar spectroscopic program if it has an i magnitude brighter than 15.0. Objects may also dropped from consideration if the photometric measurements are considered suspect, for example objects close to very bright stars, data affected by cosmic rays, etc.

One of the most important tasks during the SDSS commissioning period was to refine the quasar target selection algorithm. This selection algorithm was varied throughout the time that the EDR observations were obtained, so the objects in this catalog were not found via a uniform set of selection criteria. Indeed, some of the quasars in the catalog were not spectroscopically targeted just by the SDSS quasar selection algorithm, but rather by one of the other modules (Stoughton et al. 2002): galaxies, stars (mostly aimed at objects with the colors of unusual types of stars), optical counterparts of ROSAT sources, or serendipitous targets (again, objects of extreme colors, but defined independently from the quasar selection color limits). For a detailed discussion of the process of spectroscopic target selection, see Stoughton et al. (2002); Richards et al. (2002) discuss the final SDSS target selection criteria for quasars.

The evaluations of the survey selection efficiency (number of quasars compared to the number of quasar candidates) and completeness (fraction of quasars found by the SDSS) are complex tasks, particularly when dealing with the EDR data base; these issues, as concern future data releases, will be addressed by Richards et al. (2002). The current estimate on the efficiency of the final selection algorithm is 65-70%; the algorithm's completeness, determined from simulations and comparison with previously known quasars, should be approximately 90%. Both of these values have brightness and redshift dependences.

2.3. Spectroscopy

Spectroscopic targets chosen by the various SDSS selection algorithms (*e.g.*, quasars, galaxies, stars, serendipity) are organized onto a series of 3° diameter circular fields (Blanton et al. 2001). The positions are mapped and drilled into aluminum plates; each plate contains 640 fibers that feed two double spectrographs mounted at the Cassegrain focus of the SDSS 2.5-m telescope (see York et al. 2000 and Castander et al. 2001 for details). The spectrographs produce data covering 3800–9200 Å, with the beam split at 6150 Å by a dichroic. The data have a spectral resolution ranging from 1800 to 2100. A total of 320 fibers enter each spectrograph; each fiber subtends a diameter of 3″ on the sky, and because of mechanical constraints the centers of the fibers must be separated by at least 55″ (although in regions of sky in which plates overlap, one can have spectra of objects separated by less than this angle). Typically about 75 quasar candidate spectra among the 640 fibers are observed in a 45-minute observation (broken into three 15-minute exposures) of a field; the exposure time is increased in conditions of poor seeing or reduced sky transparency to meet survey's minimum signal-to-noise ratio requirement of $(S/N)^2$ of 15 per spectrograph pixel at $g^* = 20.2$ and $i^* = 19.9$. (See Stoughton et al. 2002 for an extensive discussion of the spectroscopic observations.)

Observations from 92 spectroscopic fields are used to form the catalog. The EDR contains 95 spectroscopic plates; of the three "missing" plates, one was a special observation of a star cluster, and the other two were duplicates of other EDR plates but drilled for observations at different airmasses. The celestial locations of the 92 plates are are displayed in Figure 1. The total area

covered by the spectroscopic observations is 494 deg^2 (as can be seen from the figure, there is significant overlap between many of the fields). The locations of the plate centers are given in Table 1, along with the number of quasars in the catalog contained on each plate. Note the wide range (10 to 123) in the number of quasars per spectroscopic plate in these commissioning observations; this variation is due to the various tests carried out during the commissioning exercise.

The data, along with the associated calibration frames, are processed by the SDSS Spectroscopic Pipeline (Burles et al., unpublished), which removes instrumental effects, extracts the spectra, determines the wavelength calibration, subtracts the sky spectrum, removes the atmospheric absorption bands, and performs the flux calibration.

The calibrated spectra are classified into various groups (e.g., star, galaxy, quasar) by another automated software pipeline (Frieman et al., unpublished). The quasar classification is based solely on the presence of broad emission lines in the spectra; the classification software does not employ information about the selection of the object (*e.g.*, was the spectrum obtained because the target selection process identified the object as a quasar candidate?), nor is luminosity used by the SDSS pipeline as a criterion for designating an object as a quasar. See Stoughton et al. (2002) for details regarding the spectral classification criteria.

The redshifts are measured by a combination of cross-correlation (using Fourier techniques) to a quasar template, and searches for emission-lines, together with code that recognizes the onset of the Lyman α forest. The software returns a redshift quality flag; when this flag indicates that a reliable redshift cannot be assigned, the redshift is measured manually. In practice, all of the quasar spectra presented herein (and the sample from which they were drawn) were visually inspected multiple times.

Figure 2 shows the calibrated SDSS spectra of six of the catalog quasars representing a wide range of properties; all were previously unknown. We discuss these individual objects in Section 5. These spectra have been slightly smoothed for display purposes.

3. Construction of the SDSS Quasar Catalog

The quasar catalog was constructed in three stages. The first step, which produced over 99% of the entries in the catalog, was simply to find the objects (4487 in total) in the EDR that the spectroscopic pipeline classified as quasars. These objects were selected using a simple SQL query to the EDR database using the SDSS Query Tool[29] (Stoughton et al. 2002). We requested all objects with spectral classifications of SPEC_QSO (`specClass=3`) or SPEC_HIZ_QSO (`specClass=4`) from the sxPrimary class of objects. For example, in SQL notation:

---

[29]http://archive.stsci.edu/sdss/software/

```
SELECT objID
FROM sxPrimary
WHERE specobj.specClass == 3 || specobj.specClass == 4
```

This query does not necessarily return *all* quasars in the EDR database, but rather it identifies all spectra that meet some well-defined criteria that cause them to belong to the sxPrimary class of objects and to be classified as quasars.

This data base was supplemented by two additional efforts. A total of 16 quasars, missed by the SDSS pipeline but identified during a visual inspection of all the EDR spectra during a search for extreme BAL quasars, were added to the quasar list. Besides BAL quasars, these objects include two star-quasar superpositions (SDSS J012412.47−010049.8 and SDSS J014349.14+002128.4) and the enigmatic object SDSS J010540.75−003314.0; see Hall et al. (2002) for a discussion of this sample.

At a late stage of the production of the catalog, a visual search of all $\approx$ 17,000 EDR spectra that were not classified as either quasars or galaxies was completed; the spectra of 61 of these sources indicated a possible AGN nature, and they were added to the initial quasar data base.

For the catalog we selected the subset of objects that 1) have at least one emission line with a FWHM that exceeds 1000 km s^{-1} and 2) have luminosities that exceed $M_{i*} = -23$. The FWHMs of the lines were determined by performing Gaussian fits to the line profiles. Note that any "narrow-lined" (Type II) quasars whose lines have FWHMs less than 1000 km s^{-1} will not be included in the catalog.

The absolute magnitudes were calculated by correcting the i^* measurement for Galactic extinction (using the maps of Schlegel, Finkbeiner, & Davis 1998) and assuming that the quasar spectral energy distribution in the ultraviolet-optical can be represented by a power law ($f_\nu \propto \nu^\alpha$), where $\alpha = -0.5$ (Vanden Berk et al. 2001). The i band was selected for the luminosity indicator rather than the more standard definition that uses the B filter primarily because of the ability of the SDSS to detect high-redshift quasars. Luminosity estimates of objects at redshifts where the Lyman α emission line is shifted redward of the observed filter are unreliable because of the absorption produced by the Lyman α forest and Lyman-limit systems; the Lyman α line does not reach the center of the i filter until redshifts of $\approx$ 5. Other advantages of the i band are 1) the flux limit of the SDSS quasar survey is set by the i band flux and 2) Galactic (and internal) reddening will be less in i than in B measurements. This definition actually matches the canonical definition of $M_B = -23$ quite well; for typical quasars, the rest frame $(B - i) \approx +0.35$. The only significant drawback to basing quasar luminosities on i rather than B is that at redshifts of a few tenths or less the luminosity calculation could be heavily influenced by the presence of a luminous stellar component rather than the quasar continuum (although note that we use point spread function magnitudes in this calculation, not Petrosian magnitudes, even for extended sources).

These criteria reduced the sample from 4564 to 3847 objects. Of the 717 objects that were dropped from the catalog, only ten were rejected solely because of the line width requirement. Of these ten objects, seven came from the second supplemental sample, which was produced by a visual inspection of the spectra and objects were included if the emission line appeared to be resolved; the other three objects, all from the original EDR quasar query, had poor quality spectra that were erroneously assigned redshifts larger than six. As expected, the vast majority of the rejected objects were low-luminosity active galactic nuclei; the SDSS images of 82% of the rejections were morphologically classified as extended sources.

The SDSS spectrum of each of the 3847 quasars was manually inspected by several of the authors. The SDSS pipeline redshifts were undoubtedly correct for over 97% of the objects; for most of the remaining spectra the redshift status flag indicated that the redshift was either uncertain or, in some cases, unknown. These spectra tended to be either of very low signal-to-noise ratio, strong (often spectacular) broad absorption line (BAL) quasars, or spectra containing only one, relatively weak, emission line.

Upon review of the spectra, a consensus was reached that it was impossible to reliably determine the redshifts of 32 objects; these were dropped from the sample (but of course are available as part of the EDR). The spectroscopic pipeline redshifts of 33 objects were significantly in error (again, most were flagged as uncertain measurements); the revised redshifts are included in this catalog. The revised redshift for one of the objects caused it to fall below the quasar luminosity cutoff. We have also revised the redshifts of many of the high-redshift ($z > 4$) quasars (usually by ≈ 0.02), as automated redshift measurements of these objects is difficult because the emission lines unaffected by the Lyman α forest either become inaccessible in the SDSS spectra or are located in regions of the spectrum with low signal-to-noise ratio; we have included the values determined in previous publications (see Anderson et al. 2001 and references therein).

As a final note, we searched for BL Lacs in the EDR by matching the FIRST catalog with the entire EDR spectroscopic data base, but after visual examination of the spectra of the candidates we did not identify any unambiguous examples of BL Lacs that are not already in the catalog.

4. Catalog Format

The first edition of the SDSS Quasar Catalog consists of 3814 quasars. The catalog is written in ASCII format and is 685 kB in size. The first 37 lines consist of catalog documentation; this is followed by 3814 lines containing information on the quasars. There are 32 columns in each line; a summary of the information is given in Table 2 (most of the catalog documentation is a repeat of Table 2).

Notes on the catalog columns:

1) The official names of the objects are given by the format SDSS Jhhmmss.ss+ddmmss.s; only

the final 18, nondegenerate characters are given in the catalog.

2-3) These columns contain the J2000 coordinates (Right Ascension and Declination) in radians. The positions for the vast majority of the objects are accurate to $0.1''$ rms in each coordinate; the largest expected errors are $0.2''$.

4) The SDSS quasar redshifts are not determined by simply using the the rest laboratory wavelengths of their emission lines, but according to the *empirical* rest wavelengths of their emission lines based upon the composite spectrum of Vanden Berk et al. (2001) assuming that [O III] represents the systemic (center of mass) redshift of the quasars. The redshifts are so determined because it is now well-known that the empirical centers of many quasar emission lines (the high ionization lines in particular) are shifted with respect to the systemic redshift of the quasars (Tytler & Fan 1992, Vanden Berk et al. 2001, and references therein). The method used by the SDSS will produce redshifts that are much closer to the systemic redshift in the ensemble average; see Stoughton et al. (2002) for more details regarding how the redshift determination is implemented. The statistical errors of the redshifts, based on either the height and width of the cross correlation function (c.f., Tonry & Davis 1979) or on the scatter of the redshifts measured from the individual emission lines, are less than 0.01 for the non-BALs and 0.01-0.03 for BAL quasars.

5) The data base search technique used to find the quasar is coded in this column. If the spectrum of the object was classified as a quasar by the SDSS software, this column contains a "0"; a "1" indicates the 16 objects identified in the extreme BAL search, a "2" is given for the 10 quasars found in the extensive visual search of EDR spectra that were not classified as either quasars or galaxies by the SDSS software.

6-15) These columns contain the magnitudes and errors for each object in the five SDSS filters. The values refer to magnitudes measured by fitting to the point spread function to the data (see Stoughton et al. 2002). Note that the quantities are asinh magnitudes (Lupton, Gunn, & Szalay 1999), which are defined by

$$m = -\frac{2.5}{\ln 10} \left[\operatorname{asinh}\left(\frac{f/f_0}{2b} \right) + \ln b \right]$$

where f_0 is the flux from a zero magnitude object and the quantity b is the softening parameter. The SDSS has set b, which is dimensionless, such that zero flux corresponds to magnitudes 24.63, 25.11, 24.80, 24.36, and 22.83 in the u, g, r, i, and z bands, respectively (Stoughton et al. 2002). For measurements that are approximately 2.5 magnitudes brighter than the zero flux values, the difference between asinh magnitudes and standard magnitudes (Pogson 1856) are less than 1%; for the vast majority of the entries in the catalog the differences between asinh and standard magnitudes are negligible (the primary exceptions being the u magnitudes of high-redshift quasars). The SDSS photometric system is normalized so that the $ugriz$ magnitudes are on the AB system (Oke & Gunn 1983).

16) Galactic absorption in the u band based on the maps of Schlegel, Finkbeiner, & Davis (1998). For an $R_V = 3.1$ absorbing medium, the absorptions in the SDSS bands are

$$A_u = 5.155 \, E(B - V)$$
$$A_g = 3.793 \, E(B - V)$$
$$A_r = 2.751 \, E(B - V)$$
$$A_i = 2.086 \, E(B - V)$$
$$A_z = 1.479 \, E(B - V)$$

17) If there is a source in the FIRST catalog within $2.0''$ of the quasar position, this column contains the FIRST peak flux density (mJy) at 20 cm.

18) The logarithm of the vignetting corrected count rate (photons s^{-1}) in the broad energy band in the following ROSAT catalogs: All-Sky Survey Faint Source Catalog (Voges et al. 2000); All-Sky Survey Bright Source Catalog (Voges et al. 1999); and the PSPC Pointing and HRI Pointing Catalogs (private communication from the ROSAT Result Archive collaboration). The matching radius was set to $60.0''$ (Faint Source Catalog), $30''$ (Bright Source Catalog and PSPC Pointings) and $10''$ (HRI Pointings); an entry of "0" in this column indicates no X-ray detection.

19) The absolute magnitude in the i band calculated assuming $H_0 = 50$, $\Omega_M = 1$, and $\Omega_\Lambda = 0$, a power law (frequency) index of -0.5, and correcting the i^* measurement for Galactic extinction.

20) If the SDSS photometric pipeline classified the image of the quasar as a point source, the catalog entry is 0; if the quasar is extended, the catalog entry is 1.

21) The version of the quasar target selection algorithm used to select the object is coded in this column ($1 = $ v2.2a, $2 = $ v2.5, $3 = $ v2.7); see Stoughton et al. (2002) for details of the different techniques.

22-27) These six columns indicate the spectroscopic target selection status for each object. An entry of "1" indicates that the object satisfied the given criterion (see Stoughton et al. 2002 for details). Note that an object can be targeted by more than one selection algorithm.

29-31) Information about the spectroscopic observation (modified Julian date, spectroscopic plate number, and spectroscopic fiber number) used to determine the redshift are contained in these columns.

32) If there is a source in the NED quasar data base within $5.0''$ of the quasar position, the NED object name is given in this column, unless the NED name refers to an SDSS-discovered object.

In addition to the catalog, the SDSS spectra of all objects in the catalog are available at a

public internet site[30].

5.   Catalog Summary

Of the 3814 objects in the catalog, 3000 were discovered by the SDSS. The 3814 quasars span a wide range of properties: redshifts from 0.15 to 5.03, $15.16 < i^* < 20.82$ (only four objects have $i^* > 20.5$), and $-30.1 < M_{i*} < -23.0$. The catalog contains 329 matches with ROSAT catalogs and 326 FIRST sources, as well as a number of unusual BAL quasars.

Figure 3 displays the i^*-redshift relation for the quasars. Previously known objects are indicated with open circles. The curved cutoff on the left hand side of the graph is due to the minimum luminosity criterion ($M_{i*} < -23$). The ridge of points just fainter than $i^* = 19$ at redshifts below three is the flux limit of the low redshift sample; low-redshift points fainter than $i^* = 19$ primarily represent objects selected via criteria other than the primary multicolor sample (*e.g.*, serendipity). Above a redshift of ≈ 3, nearly all the quasars in the catalog were discovered by the SDSS.

A histogram of the catalog redshifts is shown in Figure 4. The clear majority of the quasars have redshifts below two (the median redshift is 1.46), but there is a significant tail of objects out to a redshift of five. The dip in the curve at redshifts between 3.3 and 3.5 is due to difficulties encountered selecting these objects during the commissioning period; the final version of the target selection algorithm will significantly reduce the number of missed quasars in this redshift region.

5.1.   Analysis of Quasar Selection

A summary of the spectroscopic selection is given in Table 3. There are six selection classes, which are columns 22 to 27 in the catalog. The second column in Table 3 gives the numbers of each object that satisfied a given selection criteria, the third column contains the number of objects that were identified only by that selection class. As expected, the solid majority (81%) were selected based on the SDSS quasar selection criteria; one-third of the catalog objects were selected on that basis only. Over 60% of the quasars were identified by the serendipity code, which is also primarily an "unusual color" algorithm. About one-seventh of the catalog was selected by the serendipity criteria alone; these objects tend to be low-redshift quasars that fall below the magnitude limit of the quasar survey algorithm.

Of the 2528 quasars with $i^* < 19.0$, 2477 were found from the quasar multicolor selection; if one includes multicolor and FIRST selection, then only 20 $i^* < 19.0$ catalog quasars are missed. For the entire catalog, over 99% of the quasars are selected by either multicolor, FIRST, or

---

[30]http://archive.stsci.edu/sdss/documents/prepared_ds.html

serendipity criteria. It should be noted that the rather high fraction of faint $z < 3$ quasars selected by serendipity is not likely to be representative of future quasar target selection, as the number of quasar serendipity targets in the catalog is a result of circumstances specific to the commissioning period. We expect that the final SDSS selection algorithms, designed to produce complete samples of galaxies and quasars, will have a smaller fraction of fibers assigned to serendipitous targets than was the situation during the commissioning period.

One of the catalog entries, SDSS J114324.97−003614.5, was selected by the ROSAT algorithm but is not listed as a ROSAT source. This situation arose because during the SDSS commissioning period, the ROSAT catalogs were being upgraded; this source was included in early versions of the ROSAT catalogs but did not meet the final ROSAT selection criteria.

5.2. Bright Quasars

Fourteen of the catalog quasars have $i^* < 16.5$, but only one, SDSS J014942.50+001501.7, a $i^* = 16.24$ quasar at a redshift of 0.55, was not previously known (see spectrum in Figure 2). The catalog contains 51 quasars brighter than $i^* = 17.0$; 16 are SDSS discoveries. Four of the sixteen SDSS discoveries are FIRST sources, and seven have been detected with ROSAT.

5.3. Luminous Quasars

Of the nine catalog quasars with $M_{i*} < -28.8$ (3C 273 has $M_i = -27.3$ in our adopted cosmology), three were not previously known. SDSS J173352.23+540030.5, at $z = 3.43$ and $M_{i*} = -29.4$, is the second most luminous quasar (after HS 1700+6416 = SDSS J170100.62+641209.0) in the catalog; its spectrum is displayed in Figure 2. This object is a 7.72 mJy FIRST source. The other new highly luminous quasars are SDSS J012412.47−010049.8 ($z = 2.82$, $M_{i*} = -29.4$), and SDSS J152119.68−004818.8 ($z = 2.93$, $M_{i*} = -28.9$).

5.4. Broad Absorption Line Quasars

The catalog contains a number of BAL quasars, and it is clear that the SDSS is quite effective at finding extreme examples of this class (see Hall et al. 2002 for a discussion). One of the more spectacular examples is SDSS J172341.09+555340.5, a $z = 2.113$ low-ionization BAL quasar whose troughs have a "scalloped" appearance (see Figure 2).

5.5. Low-Redshift Quasars

The quasar with the lowest redshift in the catalog, SDSS J232259.99−005359.3 at $z = 0.15$, was not previously known (spectrum is shown in Figure 2). Of course, there are many lower-redshift AGN in the EDR that do not satisfy our luminosity criterion. Of the 49 quasars with redshifts below 0.30, 33 are reported here for the first time, as well as eight new $z < 0.20$ quasars. Included in the new discoveries are five FIRST sources and fifteen ROSAT detections. One of the low-redshift objects, SDSS J011254.91+000313.0 at $z = 0.24$, is PB 06317 in the NED data base with the erroneous redshift of $z = 1.23$.

5.6. High-Redshift Quasars

Two of the fifty $z > 3.95$ quasars in the catalog have not been previously published: SDSS J103432.71−002702.5, at $z = 4.38$, and SDSS J122657.97+000938.4, at $z = 4.14$. The spectra of both objects are displayed in Figure 2. Observations of most of the $z > 4$ quasars in the catalog were described by Anderson et al. (2001). Although only a small fraction of the objects in the catalog are at high-redshift, the SDSS is clearly very effective at discovering such quasars; 96 of the 101 catalog entries with $z > 3.5$ are SDSS discoveries.

5.7. Close Pairs

There are 14 pairs of quasars in the catalog with angular separation less than $70''$. One pair, SDSS J025959.69+004813.5 and SDSS J030000.56+004828.0, both new discoveries, have redshifts ($z = 0.893$) identical within the errors, and a separation of only $19.5''$, corresponding to a physical distance of 164 kpc; this is almost certainly a binary quasar.

5.8. Redshift Disagreements with Previous Measurements

The redshifts of twenty quasars in this catalog disagree by more than 0.07 from the values given in the NED database; the information for each of these objects is given in Table 4. All of the redshift discrepancies are larger than 0.4, and in ten of the cases the SDSS redshift is smaller than the NED. Three of the quasars in Table 4 have blank fields in the NED redshift column (identified by "..." in the third column of Table 4), and seven of the Table 4 objects are from the UM survey. The incorrect published redshifts of UM 203 and UM 183 were noted by Richards et al. (2001a).

We have reexamined the spectra of the 17 objects with actual redshift disagreements, and for all but a few the SDSS value is undoubtedly the correct one; in the cases that are not certain, we believe the SDSS redshifts are the more likely ones. Examples where the SDSS redshift could be incorrect include the two BAL quasars LBQS 0021−0100 and [HB89]2345+002, and the

2dF survey object 2QZ J130916.6−001550, where Croom et al. (2001) identify the emission line at 6900 Å as Mg II, whereas we interpret this line as Hβ and the feature near 4000 Å as Mg II emission. Note that quality flag for 2QZ J130916.6−001550 given by Croon et al. (2001) indicates an uncertain redshift.

5.9. Morphology

The SDSS photometric pipeline classifies the images of 122 quasars as resolved. As one would expect, the vast majority (87%) of the extended objects have redshifts below one, but there are a number of resolved quasars at higher redshifts (the highest redshift of an extended object is 3.61). The majority of the large redshift "resolved" quasars are probably measurement errors, but this sample probably contains a few chance superpositions of quasars and foreground objects or possibly some small angle separation gravitational lenses. A detailed study of one of the extended $z > 1$ quasars in the catalog, SDSS J122608.02−000602.2 at a redshift of 1.12, shows that the source consists of a close pair of quasars and is likely to be a gravitational lens system (Inada et al. 2002).

6. Conclusion

The current catalog contains slightly less than 5% of the planned survey area, although again we point out that the observations in the EDR were taken during the commissioning period and the final algorithm will provide more systematic study of the survey region. We plan to produce regular updates to the quasar catalog, on approximately one year intervals, throughout the duration of the survey. The next release is scheduled for late 2002; we expect it to contain more than 20,000 quasars, most identified with the final SDSS quasar selection algorithm.

---

[31]The SDSS Web site is http://www.sdss.org/.

REFERENCES

Anderson, S.F., Fan, X., Richards, G.T., Schneider, D.P., Strauss, M.A., Vanden Berk, D.E., et al. 2001, AJ, 122, 503

Becker, R.H., White, R.L., & Helfand, D.J. 1995, ApJ, 450, 559

Blanton, M.R., Lupton, R.H., Maley, F.M., Young, N., Zehavi, I., & Loveday, J. 2001, AJ, submitted

Budavari, T., Csabai, I., Szalay, A.S., Connolly, A.J., et al. 2001, AJ, 122, in press

Castander, F.J., Nichol, R.C., Merelli, A., Burles, S., Pope, A., et al. 2001, AJ, 121, 2331

Croom, S.M., Smith, R.J., Boyle, B.J., Shanks, T., Loaring, N.S., Miller, L., & Lewis, I.J., MNRAS, in press

Fan, X., Narayanan, V.K., Lupton, R.H., Strauss, M.A., et al. 2001, AJ, 122, in press

Fukugita, M., Ichikawa, T., Gunn, J.E., Doi, M., Shimasaku, K., & Schneider, D.P. 1996, AJ, 111, 1748

Gunn, J.E., Carr, M.A., Rockosi, C.M., Sekiguchi, M., et al. 1998, AJ, 116, 3040

Hall, P.B., Anderson, S.F., et al. 2002, in preparation

Hogg, D.W., Schlegel, D.J., Finkbeiner, D.P., & Gunn, J.E. 2001, AJ, 122, in press

Inada, N., Sekiguchi, M., Anderson, S.F., Burles, S., et al. 2002, in preparation

Lupton, R.H., Gunn, J.E., Ivezić, Ž., Knapp, G.R., Kent, S., & Yasuda, N. 2001, Proceedings of ADASS X, in press

Lupton, R.H., Gunn, J.E., & Szalay, A. 1999, AJ, 118, 1406

Oke, J.B., and Gunn, J.E., 1983, ApJ., 266, 713

Pogson, N.R., 1856, MNRAS, 17, 12

Richards, G.T., Fan, X., Newberg, H.J., Strauss, M.A., et al. 2002, in preparation

Richards, G.T., Fan, X., Schneider, D.P., Vanden Berk, D.E., Strauss, M.A., et al. 2001a, AJ, 121, 2308

Richards, G.T., Weinstein, M.A., Schneider, D.P., Fan, X., Strauss, M.A., Vanden Berk, D.E., et al. 2001b, AJ, 122, in press

Schlegel, D.J., Finkbeiner, D.P., & Davis, M. 1998, ApJ, 500, 525

Schmidt, M. 1963, Nature, 197, 1040

Sharp, R.G., McMahon, R.G., Irwin, J.J., & Hodgkin, S.T., 2001, MNRAS, in press

Stoughton, C., Lupton, R.H., et al. 2002, AJ, submitted

Tonry, J., and Davis, M. 1979, ApJ, 84, 1115

Tytler, D., & Fan, X. 1992, ApJS, 79, 1

Vanden Berk, D.E., Richards, G.T., Bauer, A., Strauss, M.A., et al. 2001, AJ, 122, 549

Véron-Cetty, M.P., & Véron, P. 2001, A & A, 374, 92

Voges, W., et al. 1999, A & A, 349, 389

Voges, W., et al. 2000, IAUC, 7432

York, D.G., Adelman, J., Anderson, J.E., Anderson, S.F., et al. 2000, AJ, 120, 1579

Zheng, W., Tsvetanov, Z.I., Schneider, D.P., Fan, X., et al. 2000, AJ, 120, 1607

Figure Captions

Fig. 1.— Celestial locations (equatorial, J2000) of the 92 spectroscopic plates used for the catalog. Each plate has a diameter of 3°. The total area covered by the plates is 494 deg^2.

Fig. 2.— An example of data produced by the SDSS spectrographs. The spectral resolution of the data is $\approx$ 1800; a dichroic splits the beam at 6150 Å. The data have been rebinned to 4 Å pixel^{-1} for display purposes. All six of the quasars were discovered by the SDSS. Notes on spectra: 1) SDSS J232259.99−005359.3 is the lowest redshift object in the catalog; 2) SDSS J014942.50+001501.7 is the brightest ($i^* = 16.24$) new object in the catalog; 3) SDSS J173352.23+540030.5, with $M_{i*} = -29.4$, is the second most luminous quasar in the catalog and the most luminous new object; 4) SDSS J172341.09+555340.5 is an example of an extreme BAL; 5,6) SDSS J103432.71−002702.5 and SDSS J122657.97+000938.4 are the two new $z > 4$ quasars in the catalog.

Fig. 3.— A plot of the observed i^* magnitude as a function of redshift for the 3814 objects in the catalog. Open circles indicate quasars not discovered by the SDSS.

Fig. 4.— The redshift histogram of the catalog quasars. The smallest redshift is 0.15 and the largest redshift is 5.03; the median redshift of the catalog is 1.46.

North Celestial Pole
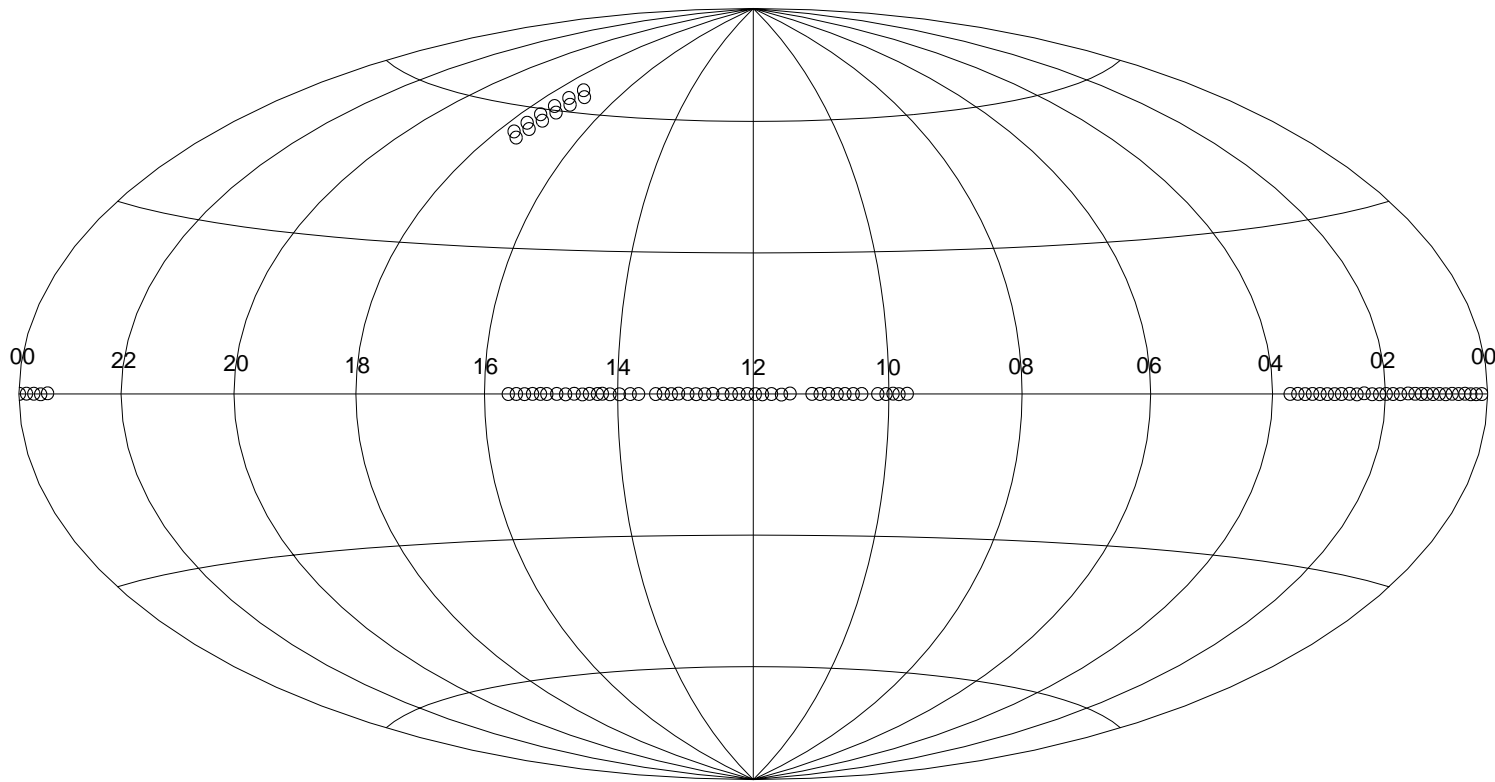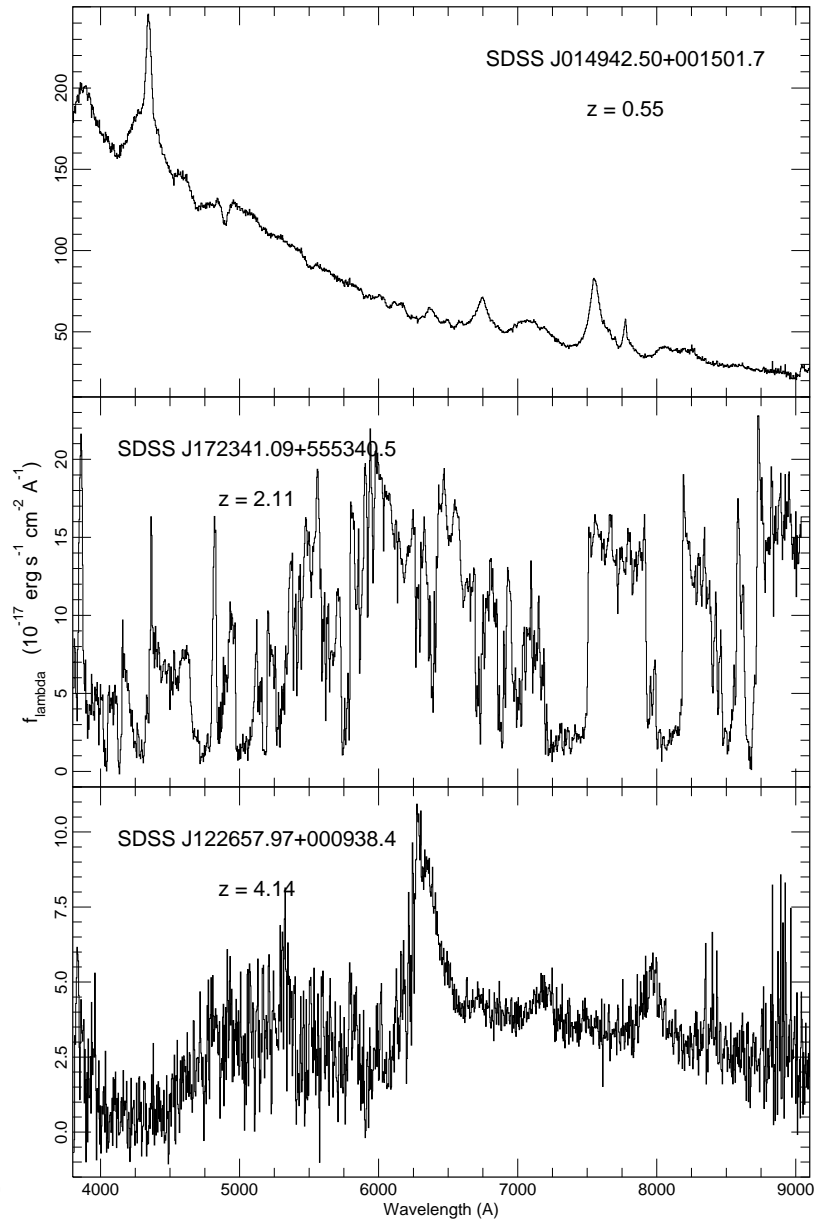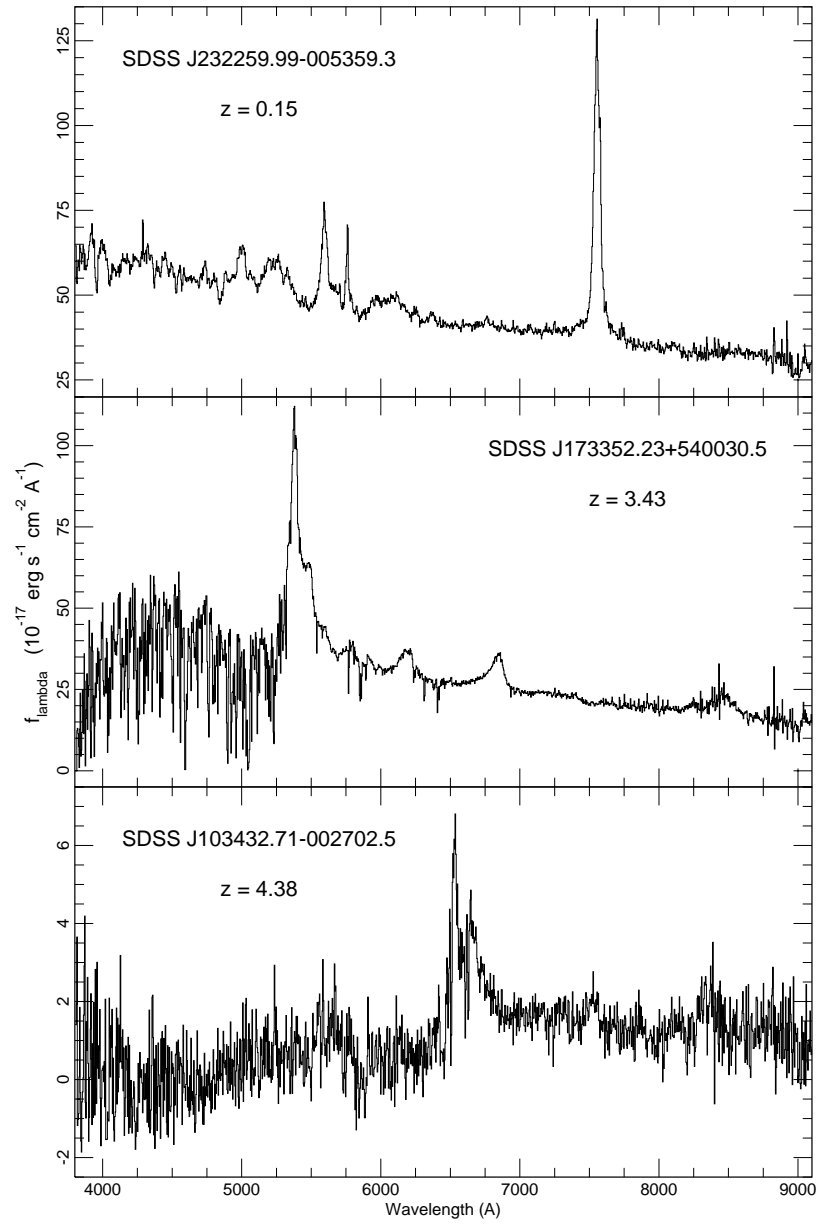
TABLE 1

SDSS Spectroscopic Plate Information

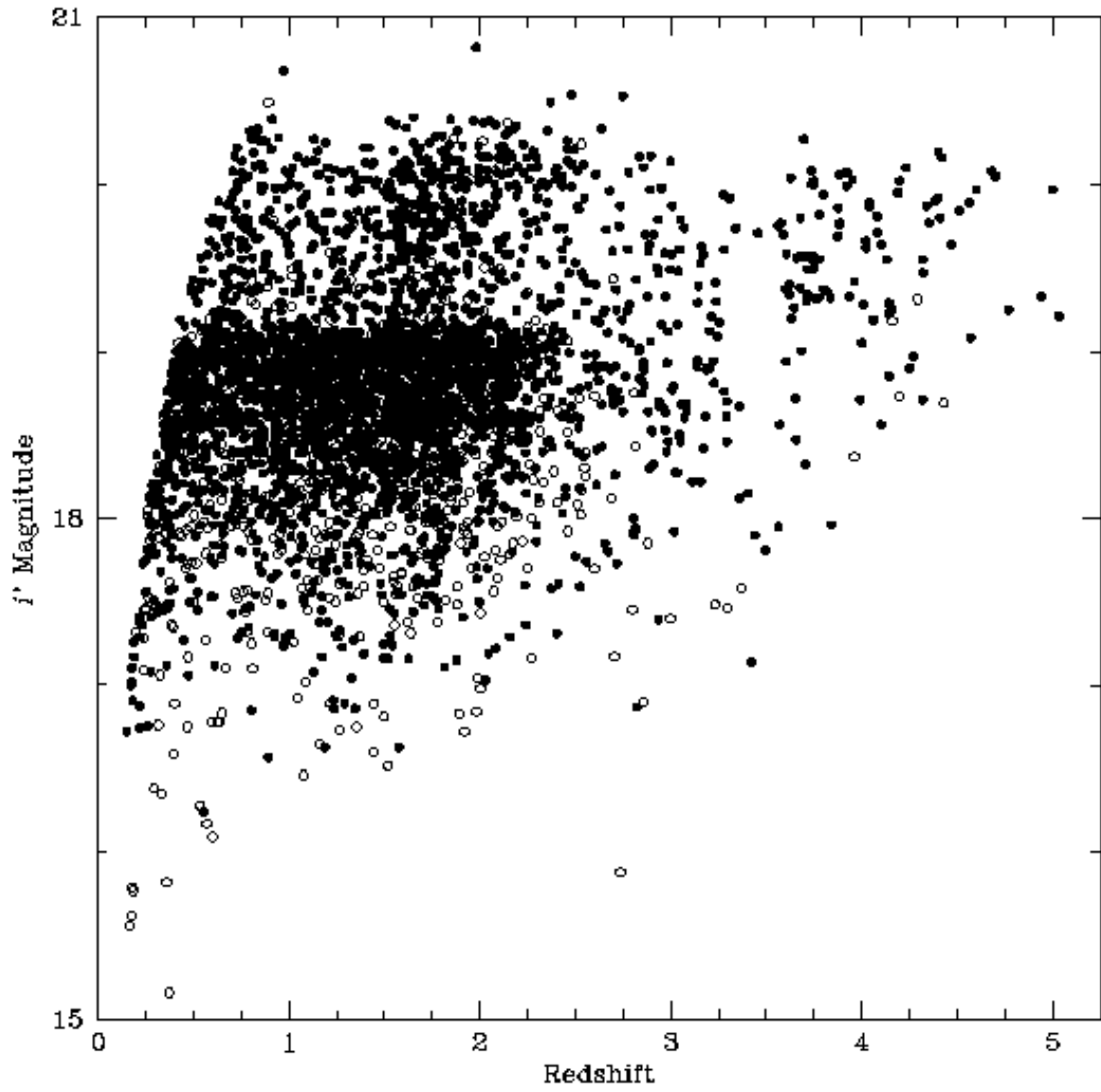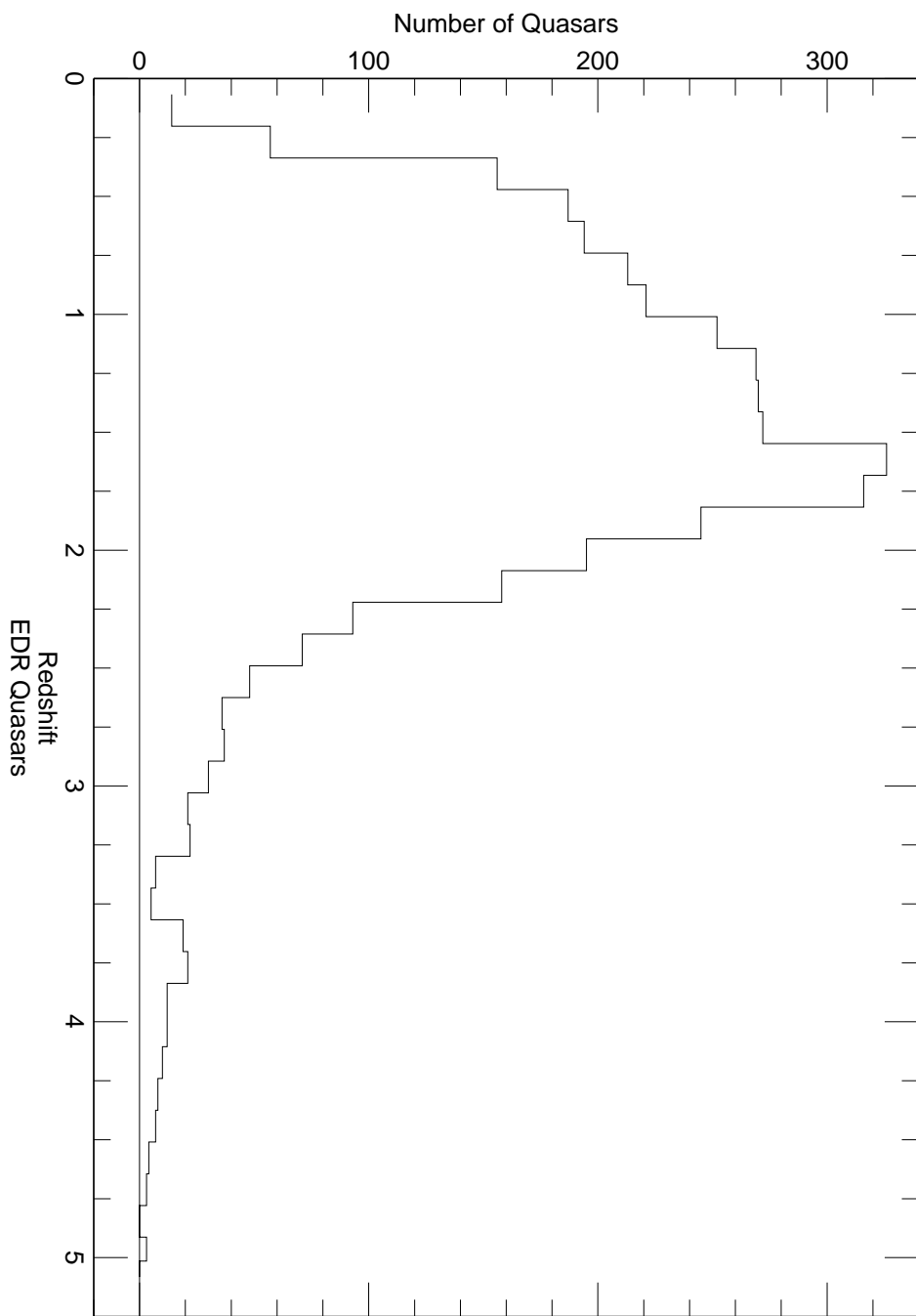| Plate	α_{2000}	δ_{2000}	N	Plate	α_{2000}	δ_{2000}	N
266	09 43 34.3	+00 03 41	24	349	16 56 34.6	+63 39 11	26
267	09 50 56.0	−00 01 50	18	350	17 13 59.4	+65 08 01	40
268	09 56 14.8	+00 04 47	12	351	17 03 48.5	+61 37 10	42
269	10 02 31.1	+00 00 00	23	352	17 20 00.3	+63 02 14	35
270	10 09 50.6	+00 00 22	17	353	17 10 08.7	+59 33 53	38
272	10 24 04.5	+00 01 06	41	354	17 25 12.6	+60 55 38	75
273	10 31 36.5	+00 00 33	45	355	17 15 44.9	+57 29 35	33
274	10 38 59.7	+00 01 06	30	358	17 33 47.8	+56 40 34	71
275	10 45 51.9	−00 00 22	29	359	17 25 14.8	+53 18 40	71
276	10 53 31.3	+00 02 34	56	360	17 37 23.6	+54 32 20	69
277	11 00 55.2	+00 00 22	38	366	17 29 45.9	+58 48 22	73
278	11 08 06.6	+00 01 39	42	367	17 20 44.9	+55 24 28	40
281	11 27 30.5	+00 06 37	34	383	23 24 48.5	+00 06 51	50
282	11 35 04.8	−00 07 10	60	384	23 33 10.8	−00 02 23	40
283	11 43 54.0	−00 00 11	54	385	23 41 33.5	+00 02 40	55
284	11 51 55.4	−00 03 52	42	386	23 50 31.7	+00 03 15	66
285	11 58 14.6	−00 00 55	29	387	23 59 17.8	+00 01 27	41
286	12 05 13.5	+00 00 33	38	388	00 07 17.9	−00 00 18	32
287	12 12 37.4	+00 01 06	36	389	00 14 14.4	−00 01 29	41
288	12 19 23.0	−00 01 06	56	390	00 20 53.5	−00 02 00	35
289	12 26 49.9	−00 01 06	53	391	00 27 59.1	+00 02 43	20
290	12 35 43.5	+00 01 50	57	392	00 35 35.0	−00 00 08	39
291	12 42 54.2	−00 02 12	26	393	00 43 16.5	+00 02 13	45
292	12 50 19.5	−00 01 28	50	394	00 50 54.6	−00 01 59	37
293	12 57 49.3	+00 00 11	66	395	00 58 26.2	+00 00 57	30
294	13 06 01.8	+00 05 20	51	396	01 05 52.9	−00 00 14	34
295	13 12 23.9	−00 01 06	30	397	01 13 04.8	+00 01 06	35
296	13 19 28.7	+00 04 03	32	398	01 19 20.5	+00 00 08	32
297	13 26 15.8	−00 00 22	26	399	01 26 40.8	+00 02 15	31
299	13 41 25.7	+00 00 22	33	400	01 34 32.8	+00 05 30	43
300	13 48 54.0	−00 00 44	45	401	01 43 17.9	−00 01 15	42
301	13 58 28.8	−00 03 19	54	402	01 51 37.5	+00 00 07	35
302	14 06 53.0	−00 02 57	42	403	01 59 16.8	+00 00 37	38
303	14 13 40.1	+00 04 03	22	404	02 06 35.0	−00 02 07	22
304	14 18 03.1	+00 00 00	29	405	02 14 43.9	−00 01 58	47
305	14 25 13.7	+00 02 01	28	406	02 23 31.9	+00 07 30	67
306	14 31 31.4	−00 04 58	34	407	02 31 23.0	−00 03 34	52
307	14 38 53.9	+00 03 19	28	408	02 39 17.4	+00 02 13	123
308	14 46 34.0	−00 03 41	39	409	02 47 59.6	+00 00 14	46
309	14 54 31.7	+00 01 28	43	410	02 55 26.8	−00 01 01	91
310	15 03 26.8	+00 00 22	39	411	03 03 08.9	−00 01 01	34
311	15 09 07.7	+00 01 28	12	412	03 10 56.2	+00 00 13	35
312	15 16 18.4	+00 01 28	26	413	03 18 44.8	+00 00 55	50
313	15 23 37.1	−00 01 17	24	414	03 26 31.5	−00 00 43	47
314	15 30 58.8	+00 00 44	10	415	03 34 05.5	+00 01 50	46
315	15 38 17.6	−00 00 11	27	416	03 41 58.0	+00 00 50	70

TABLE 2

Quasar Catalog Format

Column	Format	Description
1	A18	SDSS Object Name hhmmss.ss+ddmmss.s (J2000)
2	I10	$10000000 \times$ R.A. in radians (J2000)
3	I10	$10000000 \times$ Declination in radians (J2000)
4	I5	$1000 \times$ redshift
5	I2	0 = EDR Quasar 1 = Extreme BAL Search 2 = Visual Search
6	I5	$100 \times$ PSF u^* magnitude
7	I4	$100 \times$ error in PSF u^* magnitude
8	I5	$100 \times$ PSF g^* magnitude
9	I4	$100 \times$ error in PSF g^* magnitude
10	I5	$100 \times$ PSF r^* magnitude
11	I4	$100 \times$ error in PSF r^* magnitude
12	I5	$100 \times$ PSF i^* magnitude
13	I4	$100 \times$ error in PSF i^* magnitude
14	I5	$100 \times$ PSF z^* magnitude
15	I4	$100 \times$ error in PSF z^* magnitude
16	I5	$100 \times$ Galactic absorption in u band
17	I7	$100 \times$ FIRST Peak flux density at 20 cm (mJy)
18	I5	$-1000 \times$ log ROSAT full band count rate
19	I5	$-100 \times M_{i*}$
20	I3	Morphology flag 0 = point source 1 = extended
21	I3	Quasar Target Selection Algorithm: 1 = v2.2a 2 = v2.5 3 = v2.7
22	I3	Spectroscopic Target flag: Multicolor Quasar (0 or 1)
23	I3	Spectroscopic Target flag: FIRST (0 or 1)
24	I3	Spectroscopic Target flag: ROSAT (0 or 1)
25	I3	Spectroscopic Target flag: Serendipity (0 or 1)
26	I3	Spectroscopic Target flag: Star (0 or 1)
27	I3	Spectroscopic Target flag: Galaxy (0 or 1)
28	I6	SDSS Imaging Run Number for photometric measurements
29	I6	Modified Julian Date of spectroscopic observation
30	I5	Spectroscopic Plate Number
31	I4	Spectroscopic Fiber Number
32	A20	Object Name for previously known quasars

TABLE 3

Spectroscopic Target Selection

Class	Selected	Sole Selection
Quasar	3107	1277
FIRST	223	18
ROSAT	158	8
Serendipity	2334	549
Star	568	8
Galaxy	15	1

TABLE 4

Discrepant Redshifts

Quasar (SDSS)	$z_{\rm SDSS}$	$z_{\rm NED} - z_{\rm SDSS}$	NED Object Name
J000807.53+001619.0	1.48	−1.06	UM 203
J002411.66−004348.1	1.79	−1.02	LBQS 0021−0100
J003005.05+002848.1	1.41	+0.56	UM 248
J004319.74+005115.4	0.31	+1.69	UM 269
J011254.91+000313.0	0.24	+0.99	PB 06317
J013352.65+011345.1	0.31	+1.06	UM 338
J021558.50−005120.4	1.66	+0.71	UM 414
J021612.20−010518.9	1.49	+0.66	UM 416
J024840.98−001229.0	1.20	+0.48	US 3186
J105907.67+010303.4	1.34	...	[CCH91] 1056.6+0119
J110226.29+003553.0	0.93	...	[CCH91] 1059.9+0052
J120548.48+005343.8	0.93	−0.83	[HB89] 1203+011
J130916.67−001550.2	0.42	+1.13	2QZ J130916.6−001550
J131028.50+004408.9	1.60	...	PKS B1307+010
J234340.34+011254.4	1.95	−0.55	[HB89] 2341+009
J234506.32+010135.5	1.79	+0.91	[HB89] 2342+007
J234724.71+005246.8	1.33	−0.93	[HB89] 2344+006
J234812.39+002939.5	1.95	+1.11	[HB89] 2345+002
J235008.88−002912.6	1.14	−0.69	UM 183
J235400.41+010123.4	1.59	−1.16	ZC 2351+007A